AIP | Journal of Applied Physics

Nanoscale electromechanical properties of CaCu3Ti4O12 ceramics

R. Tararam, I. K. Bdikin, N. Panwar, J. A. Varela, P. R. Bueno et al.

Citation: J. Appl. Phys. **110**, 052019 (2011); doi: 10.1063/1.3623767
View online: http://dx.doi.org/10.1063/1.3623767
View Table of Contents: http://jap.aip.org/resource/1/JAPIAU/v110/i5
Published by the AIP Publishing LLC.

Nanoscale electromechanical properties of $CaCu_3Ti_4O_{12}$ ceramics

R. Tararam,[1] I. K. Bdikin,[2] N. Panwar,[3] J. A. Varela,[1] P. R. Bueno,[1] and A. L. Kholkin[3,a)]
[1]*Departamento de Físico-Química, Instituto de Química, Universidade Estadual Paulista (UNESP), 14800-900 Araraquara, Brasil*
[2]*Department of Mechanical Engineering & TEMA, University of Aveiro, 3810-193 Aveiro, Portugal*
[3]*Department of Ceramics and Glass Engineering & CICECO, University of Aveiro, 3810-193 Aveiro, Portugal*

(Received 16 February 2011; accepted 13 May 2011; published online 2 September 2011)

Piezoresponse Force Microscopy (PFM) is used to characterize the nanoscale electromechanical properties of centrosymmetric $CaCu_3Ti_4O_{12}$ ceramics with giant dielectric constant. Clear PFM contrast both in vertical (*out-of-plane*) and lateral (*in-plane*) modes is observed on the ceramic surface with varying magnitude and polarization direction depending on the grain crystalline orientation. Lateral signal changes its sign upon 180° rotation of the sample thus ruling out spurious electrostatic contribution and confirming piezoelectric nature of the effect. Piezoresponse could be locally reversed by suitable electrical bias (local poling) and induced polarization was quite stable showing long-time relaxation (~3 hrs). The electromechanical contrast in unpoled ceramics is attributed to the surface flexoelectric effect (strain gradient induced polarization) while piezoresponse hysteresis and ferroelectric-like behavior are discussed in terms of structural instabilities due to Ti off-center displacements and structural defects in this material. © *2011 American Institute of Physics*. [doi:10.1063/1.3623767]

INTRODUCTION

There have been intense research activities on centrosymmetric $CaCu_3Ti_4O_{12}$ (CCTO) material having body-centered cubic crystalline structure ($Im\bar{3}$ space group) since the discovery of its giant dielectric constant ($\kappa = 10^4 - 10^5$) in a radio frequency range.[1] Another important feature of CCTO is a relatively weak temperature dependence of the dielectric response (between 100–600 K) in contrast to well-known relaxor-type materials.[2,3] Several mechanisms have been proposed to explain the apparent dielectric response of CCTO. One mechanism was to attribute the unusual dielectric behavior to the extrinsic (Maxwell-Wagner type) relaxation resulting from the spatial inhomogeneity,[4] electrode effect,[5] or internal barrier layer capacitor model.[6–8] Other reports have proposed an intrinsic mechanism due to a relaxor-like dynamical slowing down of dipolar fluctuations in nanosized domains.[9] Using electron diffraction technique, Liu *et al.*[10] observed the presence of polar nanostructures in CCTO. Structural refinement suggested the existence of local dipolar moments associated with off-center displacements of Ti ions resulting in a high polarizability. The measured displacement in [001] direction of ~0.04 Å at room temperature is significant when compared with ~0.10 Å typical for ferroelectric materials. Based on this, an incipient ferroelectric behavior has been proposed for CCTO where the transition to ferroelectric state is frustrated by the tilt of TiO_6 octahedra which is required to accommodate the Cu^{2+} ions. The resultant enhanced rigidity of the octahedral framework in CCTO structure prevents the long range ordered ferroelectric state. Since macroscopic measurements provide only average information, there is an urgent need to probe polarization-dependent electromechanical properties on a nanoscale level by means of a non-destructive technique, e.g., Piezoresponse Force Microscopy (PFM) and PFM Switching Spectroscopy (PFM-SS).[11] In view of further miniaturization of the devices, the nanoscale study of polarization-dependent properties of CCTO is indispensable for the development of advanced micromechanical and microcapacitor applications.

In the present work, the local electromechanical properties of CCTO ceramics are studied by means of PFM technique[11–15] at room temperature and the results are interpreted by the contribution of the flexoelectric effect due to lattice relaxation at the ceramic surface.

Flexoelectric effect, occurring in insulating oxides, is the coupling between mechanical strain gradient and electric polarization induced by inhomogeneous strain in the materials. Strain gradients in the crystalline structure can be due to local crystal defects such as oxygen vacancies,[16] lattice relaxation at the surface and crystalline dislocations (both generating polarization instability),[17] chemical fluctuations in cationic segregation,[18] impurities,[19] and lattice mismatch of heteroepitaxial films at the substrate.[20] For a centrosymmetric crystal subjected to inhomogeneous deformation, only the strain gradient contributes to the polarization and thus the flexoelectric effect can be investigated independently.[13,21–25] Contrary to ferroelectric polarization that occurs in the whole crystalline structure in non-centrosymmetric crystals, flexoelectric polarization is localized in the volumes with broken symmetry subjected to inhomogeneous deformation (Fig. 1). The impact of flexoelectric effect can be significant in the cases where the global polarization is absent on the macroscopic scale and in nanostructures.[26]

EXPERIMENTAL PROCEDURES

The stoichiometric CCTO polycrystalline samples were prepared by conventional solid-state reaction route. All the starting chemicals were of analytical grade: $CaCO_3$ (Aldrich-99%),

a)Author to whom correspondence should be addressed. Electronic mail: kholkin@ua.pt.

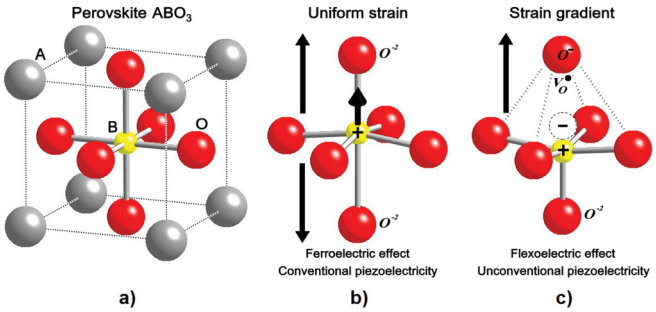

FIG. 1. (Color online) (a) ABO_3 cubic perovskite structure showing (b) the uniform strain in the crystalline cell with ferroelectric polarization and (c) flexoelectric induced polarization due to strain gradient.

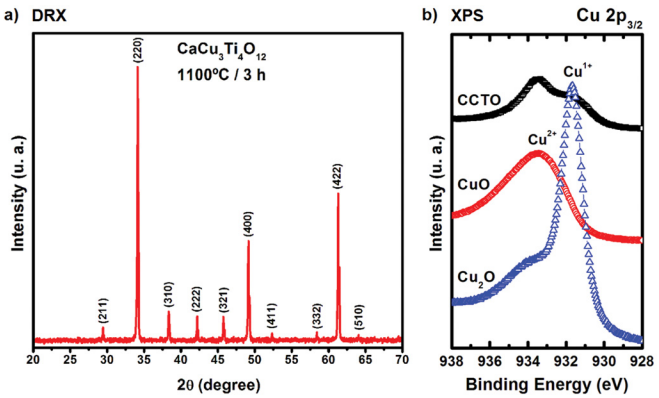

FIG. 2. (Color online) (a) X-ray diffraction and (b) x-ray photoelectron spectroscopy of CCTO material sintered at 1100 °C for 3 h.

TiO_2 (Aldrich-99.8%) and CuO (Riedel-99.9%), using appropriate molar mixing to reach CCTO stoichiometry. These oxides were milled in alcohol for 24 h with zirconia balls inside a polyethylene bottle. The slurry was dried and heat-treated at 900 °C in an ambient atmosphere for 12 h. The heat-treated powders were uniaxially pressed (1 MPa) into pellets of 10 mm in diameter and 1 mm thickness followed by isostatic pressing at 210 MPa. The pellets were further sintered at 1100 °C for 3 h in a conventional furnace under ambient atmosphere with heating and cooling rates of 5 °C/min. The sintered sample was carefully polished until the faces became smooth and flat for both microstructure and spectroscopic measurements.

The polished samples were characterized by x-ray diffraction (XRD, Rigaku 20-2000) using Cu K α radiation. X-ray photoelectron spectrum (XPS) of CCTO polished samples was recorded by VG-Escalab spectrometer with Cu K α radiation. The results were processed with a CasaXPS software and the binding energies were corrected using the component of C 1s (from hydrocarbons adsorbed onto the sample's surface) fixed at 284.6 eV. This procedure was used to verify the oxidation state of the sample with standard Cu I and II patterns.

PFM capabilities were implemented using commercial Atomic Force Microscopy (AFM, Multimode, NanoScope IIIA, Bruker and NT-MDT, Ntegra Aura). For image acquisition and local polarization measurements in PFM mode, the microscopes were equipped with external lock-in amplifier (SR-830, Stanford Research), function generator (FG120, Yokogawa), and voltage amplifier (7602, Krohn-Hite). PFM images of polished sample were obtained by applying ac voltage (30–45 V, peak-to-peak) with frequency of 50 kHz (*out-of-plane*) and 5 kHz (*in-plane*). The topographic images were simultaneously acquired. Conductive probes (stiffness 42 N/m, resonance frequency 300 kHz, PPP-NCHR, Nanosensors) were used for the PFM and PFM-SS measurements in ambient conditions. The tip has the shape of a polygon-based pyramid with the height of 10–15 μm and the effective radius $\approx$10 nm. The cantilever response due to electromechanical coupling was detected by conventional configuration of the lock-in and auxillary channels of the AFM.[13,14,27]

RESULTS AND DISCUSSION

Figure 2(a) shows the x-ray diffraction pattern of sintered CCTO powder where all characteristic diffraction peaks corresponding to the cubic crystalline phase of $CaCu_3Ti_4O_{12}$ were identified without any secondary phase. In order to probe the oxidation state copper, the XPS method was used and the results are presented in Fig. 2(b). There is an asymmetry in Cu $2p_{3/2}$ peak for CCTO with the main component at 933.5 eV corresponding to Cu^{2+} using CuO (copper II) as a reference, whereas the lower binding energy contribution around 931.7 eV is related to the presence of Cu^{1+} using Cu_2O (copper I).[28] Cu^{1+}, likely formed during high temperature sintering process, was not apparently detected by XRD technique as a Cu_2O secondary phase. It is, therefore, assumed that Cu^{1+} is present in the CCTO crystalline structure as a point defect substituting Cu^{2+} and forming Cu'_{Cu} structural imperfections.

It is well known that Cu^{2+} is a d^9 transition ion and is able to cause Jahn-Teller distortions due to the presence of odd number of electrons in e_g orbital.[29,30] In dodecahedron sites of CCTO, Cu^{2+} presents four short bondings which decreases the electronic cloud symmetry in the cluster $[CuO_{12}]$, leading to the distortion and tilt of TiO_6 octahedron. Substitution of Cu^{2+} by Cu^{1+} as a defect, leads to a higher symmetry of the electronic cloud in the negative clusters $[CuO_{12}]$ because the latter is a d^{10} ion which prohibits Jahn-Teller effect. In order to maintain the charge neutrality, Cu^{1+} formation would lead to the formation of TiO_5 clusters and oxygen vacancies [Fig. 1(c)].[31,32] The oxygen vacancies would be easily accommodated in the TiO_5 local substructure. Thus, the increasing of Cu-O bonding causes structural disorder in the TiO_6 octahedron network. The charge transfer between TiO_5. $V_O^{\bullet}$ clusters and Cu'_{Cu} defects creates positive and negative polarons and the combination of both constitutes a new entity called Jahn-Teller bipolaron that causes additional strain. This may lead to ferroelectric-like properties as discussed in the following.

We investigated the nanoscale electromechanical properties in CCTO by means of PFM since this technique allows the control and manipulation of the polarization confined near the surface. Experimentally, the application of an ac electric bias to the surface induces an oscillating electrical field in the material, resulting in a local deformation due to piezoelectric effect. However, if the piezoelectric coefficient is small as frequently observed in macroscopically non-polar materials (e.g., in $SrTiO_3$ (Ref. 13) and $(La,Sr)MnO_3$),[33]

other effects like vacancies electromigration[34] or apparent electrostriction may also play a role and nanoscale electromechanical response may be a combined effect of all these. For instance, at high ac voltage applied to study piezoeffect, electrostriction may be significant giving rise to the 2nd harmonic of the electromechanical signal. Signal obtained from lock-in amplifier provides information of the deflection amplitude of the cantilever, i.e., $A_{1\omega}$ (first harmonic) and phase (θ) of the oscillation leading to z coordinates of the piezoresponse image $PR = aA_{1\omega}\cos\theta/V_{ac}$ with the scale unit in volts (V) and a is the calibration constant. The calibration constant depends on the lock-in and photodiode sensitivity to the surface vibrations.[11] The piezoresponse amplitude defines the local electromechanical activity of the surface and the phase signal depends on the orientation of polarization vector. Figure 3 displays representative PFM images of the polished CCTO surface. From the topographic image [Fig. 3(a)], it is possible to differentiate the polycrystalline grains of CCTO along with the presence of low concentration of topographic defects due to polishing. PFM images could be obtained under sufficiently high ac voltage ($V_{ac} = 45$ V) due to the very low piezoelectric coefficients (much lower than in typical ferroelectrics).[14,27] In *out-of-plane* or vertical PFM (VPFM) image shown in Fig. 3(b), the contrast is associated with the direction of the intragrain polarization. Here, the bright regions correspond to domains with the polarization vector oriented toward the bottom electrode and referred as down polarization. Dark regions correspond to domains oriented upward (referred herewith as up polarization). The observed PFM signal is roughly uniform within the grains, but differs from grain to grain in magnitude (value of the corresponding effective piezoelectric coefficient) and in direction (phase of the signal). The enhanced piezoresponse at the grain boundaries may be attributed to the inhomogeneous distribution of oxygen vacancies similar to the case of $SrTiO_3$ ceramics.[13] It should be noted that the PFM contrast is obtained for both VPFM and lateral (LPFM) deflections of the cantilever signal during scanning as a result of surface longitudinal and shear deformations, respectively. Therefore, VPFM provides information about *out-of-plane* polarization component, perpendicular to the sample's surface and is proportional to the effective d_{33} piezoelectric coefficient. On the other hand, LPFM yields *in-plane* polarization component, parallel to the sample's surface. Two in-plane piezoresponse images [Figs. 3(c) and 3(d)], x-LPFM and y-LPFM (sample rotated at 90°), provide information about the absolute value of the effective shear d_{15} piezoelectric coefficients. Therefore, all three components of polarization vector can be obtained in CCTO ceramics. The piezoelectric coefficients d_{33} is defined by the relation

$$d_{33} = 2\,\varepsilon_0\, Q_{eff} P_s \varepsilon, \tag{1}$$

where P_s is the spontaneous polarization, Q_{eff} is the electrostriction coefficient, ε_0 is the permittivity of vacuum, and ε is the relative dielectric permittivity (approximately 10^4). The average piezoelectric coefficient d_{33} based on the measured piezoresponse images (using PZT films as reference) is 2.6 pm/V. From Eq. (1), $P_s = 0.08\ \mu\text{C/cm}^2$ (we have taken $Q_{\text{eff}} \sim 1.8 \times 10^{-2}\ \text{m}^4/\text{C}^2$ (Ref. 35)). Further, $P_s \sim P_m^f = f_{mnop}\,\delta s_{no}/\delta x_p$ is the flexoelectric polarization determined by the strain gradient $\delta s_{no}/\delta x_p$ and the tensor of flexoelectric coefficients f_{mnop}. It should be mentioned that the matrix of the induced piezoelectric coefficients has to be rotated in accordance with the orientation of a particular grain. As in the case of CCTO strain gradient near the surface is not known, we approximated its value to be $2.5 \times 10^2\ \text{m}^{-1}$ (based on the value reported for $SrTiO_3$ (Ref. 36) exhibiting also the surface flexoelectric effect). Spontaneous polarization for CCTO based on the measured average piezoelectric coefficients was $0.08\ \mu\text{C/cm}^2$. Thus the average absolute value of the flexoelectric coefficient for CCTO is of the order of $3.2\ \mu\text{C/m}$, comparable to that for lead zirconate titanate ceramics.[37]

In order to further confirm the piezoelectric nature of the obtained images (and to rule out the possible contribution of electrostatic component to the PFM signal[38]), we measured the *in-plane* contrast for two different orientations of the sample. Figures 4(a) and (b) show the topographical and x-LPFM images for a specific sample's region whereas Fig. 4(c) presents x-LPFM image of same region after the rotation of the sample at 180° around the axis normal to the

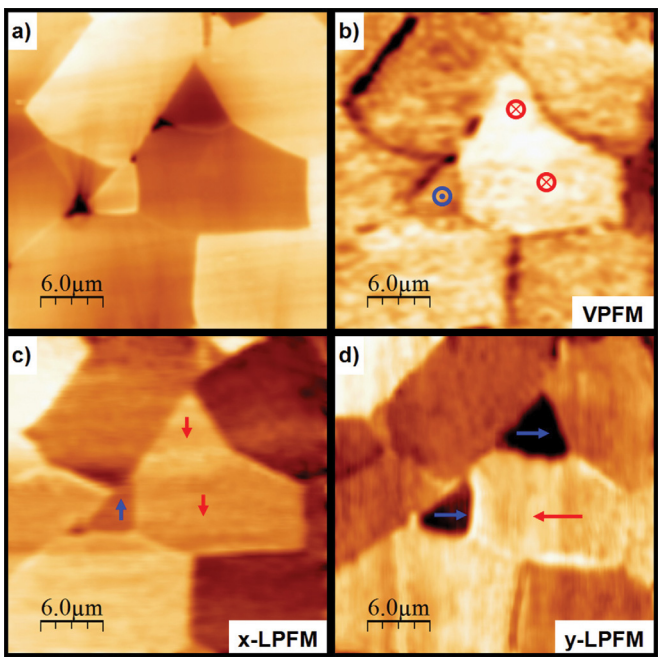

FIG. 3. (Color online) (a) Topography, (b) out-of-plane PFM (VPFM), (c) in-plane PFM (x-LPFM), and (d) in-plane PFM after 90° rotation (y-LPFM) piezoresponse contrasts of the CCTO sample with applied voltage $V_{ac} = 45$ V. The arrows show projections of polarization on axes x, y, and z.

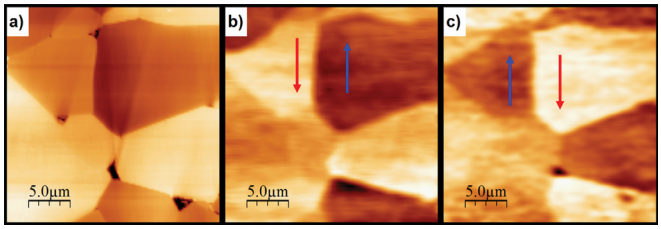

FIG. 4. (Color online) (a) Topographic images of CCTO sample, (b) x-LPFM, and (c) x-LPFM of the same local after rotation of sample at 180°. Piezoelectric contrast of grains is reversed.

surface. Sample rotation does not change the topography and electrostatic cross-talk, but, on the other hand, it should change the sign of the in-plane piezoresponse (reverse contrast to the opposite). It follows from Figs. 4(b) and (c) that the sample rotation at 180° indeed changes the phase of the signal to the opposite, therefore, attesting that the true electromechanical response from the sample is acquired.

The PFM contrast from the CCTO sample was complemented by the local piezoelectric hysteresis loop measurement in different CCTO grains to verify the behavior of the surface polarization under the applied electric bias. Switching spectroscopy PFM in the so-called pulse mode was used to obtain hysteresis curves.[39] This methodology consists of applying dc voltages, V_{dc}, for a short time (~0.5 s). The VPFM signal proportional to the d_{33} is measured between the increasing voltage pulses (periods of ~2 s) with increments of 0.1 V. Sufficiently high ac voltages (30 V peak-to-peak) and frequency of 50 kHz was used for loop acquisition. Figure 5 shows the piezoelectric hysteresis loops obtained in the fixed location in the center of the CCTO grain. The behavior is representative for different areas and grains. The measurements were done in a dc voltage range -30 V $\leq V_{dc} \leq +30$ V that correspond to a very high local electric field concentrated under the tip (inset to Fig. 5). It can be seen that the vertical component of the polarization is fully reversible with bias having coercive voltages of around ±10 V and saturation achieved at ±30 V for both polarities of the applied bias. The gap in the 1st hysteresis cycle is likely to indicate that higher local polar ordering can be achieved as compared to zero-field polarization (presumably of the flexoelectric origin). This behavior is typical for ferroelectric relaxors where a similar shape of the hysteresis was indeed observed.[40,41] In this context it should be noted that the narrow polarization-electric field hysteresis loops were also reported in CCTO[42,43] but these were less square due to apparently lower electric field in the macroscopic configuration.

Switching by PFM has also been confirmed with the local poling performed by the tip. The reversible orientation

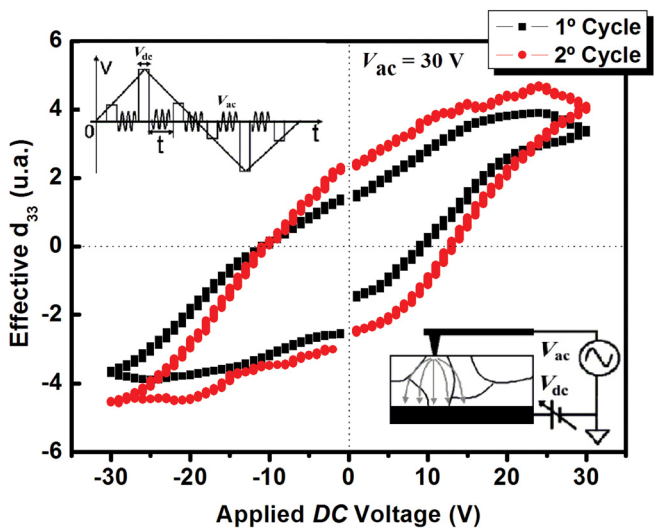

FIG. 5. (Color online) Local piezoelectric hysteresis loops of CCTO sample.

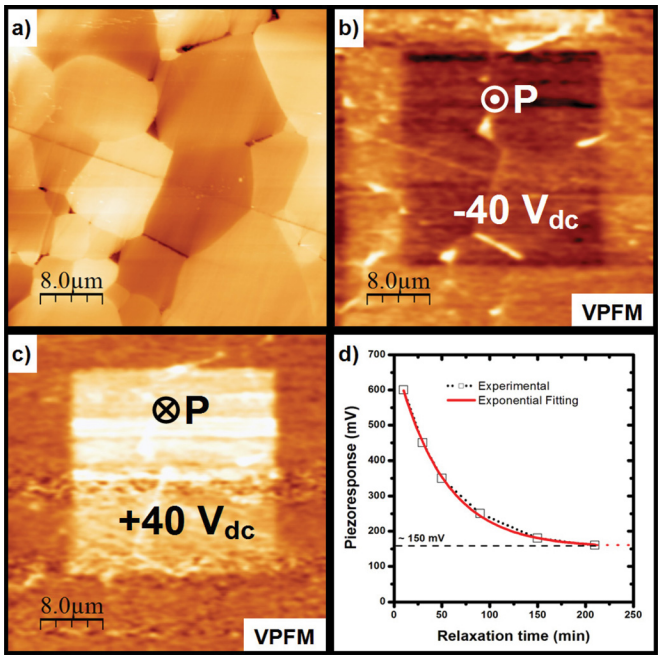

FIG. 6. (Color online) (a) Topographic images of CCTO sample and local poling results under (b) −40 V and (c) + 40 V. In (d) exponential polarization decay up to equilibrium state has been verified.

of local polarization induced in CCTO ceramics could be also reproduced on a larger area of the sample. The VPFM images presented in Fig. 6 show a 25×25 μm^2 area of local poling inside an area of 40×40 μm^2 [topographical image in Fig. 6(a)]. The piezoresponse images of negative and positive polarized regions have been obtained after applying a tip bias of −40 V [Fig. 6(b)], and then an opposite bias of +40 V [Fig. 6(c)]. High dc voltage (much higher than the coercive one) was used to create two opposite directions of polarization. The contrast difference between the bright and dark areas reconfirms the reorientation polarization vector perpendicular to the ceramic surface irrespectively of their initial polarization direction. These results demonstrate that the stable polarization patterns can be written on the CCTO grains which persist for long time (at least 3 hrs) after polarization exponential decay [Fig. 6(d)]. This value of relaxation time is several orders of magnitude greater than that calculated using Maxwell-Wagner relation ($\tau = 4\ \pi\ \varepsilon\ \varepsilon_o/\sigma$, where σ is the electrical conductivity of CCTO $\sim 10^{-9}$ $(\Omega cm)^{-1}$,[44] and $\varepsilon = 10^4$, therefore, the relaxation time based on this relation is ~1 s). This indicates that the locally induced charged states decay with the characteristic time that is many orders of magnitude greater than the charge relaxation and might be attributed to induced ferroelectric polarization. The polaron defects associated with stacking faults may be responsible for the high polarization value as was recently reported by Bueno *et al.*[31] Flexoelectric polarization at the surface is the natural consequence of high polarizability.

CONCLUSIONS

Piezoelectric contrast is observed in CCTO ceramics using PFM technique. The measurements were performed to map the 3D polarization vector with varying amplitude and

direction according to the grain crystalline orientation. This polarization is attested to the surface flexoelectric effect. Local switching after high voltage poling combined with hysteresis loops acquisition confirms the intrinsic nature of polarizability and is discussed in terms of ferroelectric-like frustrated state. It was considered that such effect has its origin associated to the presence of polar clusters related to structural disorder via, e.g., stacking faults. We believe that the observed electromechanical response is an important feature that enables CCTO materials to be used in micromechanical applications.

ACKNOWLEDGMENTS

The authors gratefully acknowledge the financial support of the Brazilian research funding agency FAPESP and CNPq. The authors are also very grateful to Peter Hammer for XPS facilities and measurements. One of the authors (N.P.) would like to thank Portuguese Foundation for Science and Technology for the financial support through postdoctoral grant (SFRH/BPD/ 71289/2010).

[1]M. A. Subramanian, D. Li, N. Duan, B. A. Reisner, and A. W. Sleight, J. Solid State Chem. **151**, 323 (2000).
[2]T. Adams, D. Sinclair, and A. West, Phys. Rev. B **73**, 094124 (2006).
[3]J. L. Zhang, P. Zheng, C. L. Wang, M. L. Zhao, J. C. Li, and J. F. Wang, Appl. Phys. Lett. **87**, 142901 (2005).
[4]M. H. Cohen, J. B. Neaton, L. X. He, and D. Vanderbilt, J. Appl. Phys. **94**, 3299 (2003).
[5]P. Lunkenheimer, R. Fichtl, S. G. Ebbinghaus, and A. Loidl, Phys. Rev. B **70**, 172102 (2004).
[6]D. C. Sinclair, T. B. Adams, F. D. Morrison, and A. R. West, Appl. Phys. Lett. **80**, 2153 (2002).
[7]T. B. Adams, D. C. Sinclair, and A. R. West, Adv. Mater. **14**, 321 (2002).
[8]S. Y. Chung, I. D. Kim, and S. J. L. Kang, Nat. Mater. **3**, 774 (2004).
[9]C. C. Homes, T. Vogt, S. M. Shapiro, S. Wakimoto, and A. P. Ramirez, Science **293**, 673 (2001).
[10]Y. Liu, R. L. Withers, and X. Y. Wei, Phys. Rev. B **72**, 134104 (2005).
[11]S. V. Kalinin, N. Setter, and A. L. Kholkin, MRS Bulletin **34**, 634 (2009).
[12]S. V. Kalinin, R. Shao, and D. A. Bonnell, J. Amer. Ceram. Soc. **88**, 1077 (2005).
[13]A. Kholkin, I. Bdikin, T. Ostapchuk, and J. Petzelt, Appl. Phys. Lett. **93**, 222905 (2008).
[14]A. Kholkin, S. Kalinin, A. Roelofs, and A. Gruverman, in *Scanning Probe Microscopy: Electrical and Electromechanical Phenomena at the Nanoscale*, Vol. 1, S. Kalinin and A. Gruverman eds. (Springer Science & Business Media, New York, 2007), p. 173.
[15]A. Gruverman and S. V. Kalinin, J. Mat. Sci. **41**, 107 (2006).
[16]J. F. Scott and M. Dawber, Appl. Phys. Lett. **76**, 3801 (2000).
[17]M. W. Chu, I. Szafraniak, R. Scholz, C. Harnagea, D. Hesse, M. Alexe, and U. Gosele, Nat. Mater. **3**, 87 (2004).
[18]J. L. Maurice, F. Pailloux, A. Barthelemy, O. Durand, D. Imhoff, R. Lyonnet, A. Rocher, and J. P. Contour, Phil. Mag. **83**, 3201 (2003).
[19]D. Balzar, P. A. Ramakrishnan, and A. M. Hermann, Phys. Rev. B **70**, 092103 (2004).
[20]G. Catalan, B. Noheda, J. McAneney, L. J. Sinnamon, and J. M. Gregg, Phys. Rev. B **72**, 020102 (2005).
[21]G. Catalan, L. J. Sinnamon, and J. M. Gregg, J. Phys.: Cond. Matter. **16**, 2253 (2004).
[22]A. K. Tagantsev, Phys. Rev. B **34**, 5883 (1986).
[23]W. Ma and L. E. Cross, Appl. Phys. Lett. **79**, 4420 (2001).
[24]W. H. Ma and L. E. Cross, Appl. Phys. Lett. **81**, 3440 (2002).
[25]P. Zubko, G. Catalan, A. Buckley, P. R. L. Welche, and J. F. Scott, Phys. Rev. Lett. **99**, 167601 (2007).
[26]E. A. Eliseev, A. N. Morozovska, M. D. Glinchuk, and R. Blinc, Phys. Rev. B **79**, 165433 (2009).
[27]A. L. Kholkin, I. K. Bdikin, V. V. Shvartsman, and N. A. Pertsev, Nanotechnology **18**, 095502 (2007).
[28]L. Ni and X. M. Chen, Appl. Phys. Lett. **91**, 122905 (2007).
[29]J. B. Goodenough, Ann. Rev. Mat. Sci. **28**, 1 (1998).
[30]K. A. Muller, J. Supercond. **12**, 3 (1999).
[31]P. R. Bueno, R. Tararan, R. Parra, E. Joanni, M. A. Ramirez, W. C. Ribeiro, E. Longo, and J. A. Varela, J. Phys. D: Appl. Phys. **42**, 055404 (2009).
[32]E. Orhan, J. A. Varela, A. Zenatti, M. F. C. Gurgel, F. M. Pontes, E. R. Leite, E. Longo, P. S. Pizani, A. Beltran, and J. Andres, Phys. Rev. B **71**, 085113 (2005).
[33]R. F. Mamin, I. K. Bdikin, and A. L. Kholkin, Appl. Phys. Lett. **94**, 222901 (2009).
[34]N. Balke, S. Jesse, A. N. Morozovska, E. Eliseev, D. W. Chung, Y. Kim, L. Adamczyk, R. E. Garcıa, N. Dudney, and S. V. Kalinin, Nature Nanotech. **5**, 749 (2010).
[35]R. Pirc, R. Blinc, and V. S. Vikhnin, Phys. Rev. B **69**, 212105 (2004).
[36]J. Petzelt, T. Ostapchuk, I. Gregora, I. Rychetsky, S. Hoffmann-Eifert, A. V. Pronin, Y. Yuzyuk, B. P. Gorshunov, S. Kamba, V. Bovtun, J. Pokorny, M. Savinov, V. Porokhonskyy, D. Rafaja, P. Vanek, A. Almeida, M. R. Chaves, A. A. Volkov, M. Dressel, and R. Waser, Phys. Rev. B **64**, 184111 (2001).
[37]W. Ma, Phys. Scripta **T129**, 180 (2007).
[38]S. V. Kalinin and D. A. Bonnell, Phys. Rev. B **63**, 125411 (2001).
[39]A. Wu, P. M. Vilarinho, V. V. Shvartsman, G. Suchaneck, and A. L. Kholkin, Nanotechnology **16**, 2587 (2005).
[40]V. V. Shvartsman, A. Yu. Emelyanov, A. Safari, and A. L. Kholkin, Appl. Phys. Lett. **81**, 117 (2002).
[41]I. K. Bdikin, V. V. Shvartsman, and A. L. Kholkin, Appl. Phys. Lett. **83**, 4232 (2003).
[42]S. M. Ke, H. T. Huang, and H. Q. Fan, Appl. Phys. Lett. **89**, 182904 (2006).
[43]B. S. Prakash and K. B. R. Varma, Appl. Phys. Lett. **90**, 082903 (2007).
[44]C.-M. Wang, S.-Y. Lin, K.-S. Kao, Y.-C. Chen, and S.-C. Weng, J. Alloys Compd. **491**, 423 (2010).